

1 **Soil erodibility ~~estimation by using five methods~~ and its influencing factors on the Loess Plateau of**

2 **~~estimating K value~~China: A case study in the Ansai watershed ~~of Loess Plateau, China~~**

3 **Wenwu Zhao, Hui Wei, ~~Lizhi Jia~~, Stefani Daryanto, Xiao Zhang, Lizhi Jia, Yanxu Liu**

4 State Key Laboratory of Earth Surface Processes and Resources Ecology, Faculty of Geographical Science,

5 Beijing Normal University, Beijing 100875, China

6 Institute of Land Surface System and Sustainable Development, Faculty of Geographical Science, Beijing

7 Normal University, Beijing 100875, China

8 *Correspondence to:* Wenwu Zhao (Zhaoww@bnu.edu.cn)

9 **Abstract**

10 The objectives of this work were to ~~select~~identify the possible best ~~texture-based~~ method to estimate soil erodibility
11 (K) and understand ~~possible indirect environmental~~the influencing factors of soil erodibility. In this study, 151 soil
12 samples were collected during soil surveys in the Ansai watershed. ~~Five methods~~ of ~~estimating K value were used~~
13 ~~to estimate soil erodibility, including the~~the Loess Plateau of China. The K values were estimated by five methods:
14 erosion-productivity impact model (EPIC), ~~the~~ nomograph equation (NOMO), ~~the~~ modified nomograph equation
15 (M-NOMO), ~~the~~ Torri model and ~~the~~ Shirazi model. The main conclusions of this paper are (1) K values in the
16 Ansai watershed ranged between 0.009 and 0.092 t·hm²·hr/(MJ·mm·hm²). ~~The K values based on Torri, NOMO,~~
17 ~~and Shirazi models were similar), and the maximum values were 1.872-7.333 times larger than the corresponding~~
18 minimum values, and were located close to each other in the Taylor diagrams. By combining the measured soil
19 erodibility, we suggested Shirazi and Torri model as models were considered the optimal models for the Ansai
20 watershed. (2) Different land use types had different levels of importance; PC accounted for 100% (native
21 grassland), 48.88% (sea buckthorn), 62.05% (Caragana korshinskii) and 53.61% (pasture grassland) of the
22 variance in soil erodibility. (3) The correlations between soil erodibility and the selected environmental variables

23 ~~changed for~~differed among different vegetation ~~typetypes~~. For native grasslands, soil erodibility had significant
24 correlations with terrain factors. For the most artificially managed vegetation types (e.g., apple orchards) and
25 artificially restored vegetation types (e.g., sea buckthorn), ~~the~~ soil erodibility had significant correlations with the
26 growing conditions of vegetation. ~~The dominant factors that influenced soil erodibility differed with different~~
27 ~~vegetation types~~. Soil erodibility had indirect ~~relationship with~~relationships not only with environmental factors
28 (e.g., elevation and slope);), but also human activities,), which potentially altered soil erodibility.

29 **Keywords:** Influencing factors, Soil erodibility, Variation features, Shirazi model, Torri model

30 **1 Introduction**

31 Soil erodibility (K), ~~as~~ one of the key factors of soil erosion (Igwe, 2003; Fu et al., 2005; Ferreira et al., 2015),
32 is defined as the susceptibility of soil to erosional processes (Bagarello et al., 2012; Bryan et al., 1989). It has been
33 extensively used in both theoretical and practical approaches to measure soil erosion. ~~Yet~~However, it is a complex
34 concept ~~and is~~ affected by many factors, including soil properties (~~e.g., soil texture, permeability and structural~~
35 ~~stability~~) (Chen et al., 2013; Wang et al., 2015; Manmohan et al., 2012);), terrain (Wang et al., 2012; Mwaniki et
36 al., 2015; Parajuli et al., 2015);), climate (Hussein et al., 2013; Sanchis et al., 2010);), vegetation (Sepúlveda-
37 Lozada et al., 2009);), and land use (Cerdà et al., 1998; Tang et al., 2016). ~~In order to~~To calculate soil erodibility,
38 many strategies have been used to perform ~~research~~researches to understand soil erodibility, including
39 measurements of physical and chemical soil properties, instrumental measurements, mathematical models and
40 graphical methods (Wei et al., ~~2017~~2017a). Although ~~at~~the direct measurement of soil erosion within large plots
41 under natural rainfall over long-term ~~period~~periods can provide ~~more~~ accurate estimates of soil erodibility, this
42 method is time consuming and ~~very expensive~~costly (Bonilla et al., 2012; Vaezi et al., 2016a, b). Therefore,
43 mathematical models are more commonly used to estimate soil erodibility.

44 Some of the most common estimation models are the nomogram model (NOMO) and the modified nomogram

45 model, (M-NOMO), which were established by Wischmeier (Wischmeier et al., 1971, 1978); the erosion-
46 productivity impact model (EPIC), which was developed by Williams (Williams et al., 1990); the best nonlinear
47 fitting formula using the physical and chemical properties of the soil, which was developed by Torri (Torri et al.,
48 1997); and the estimation model developed by Shirazi that ~~is using~~uses the average size of the soil geometry
49 (Shirazi et al., 1988). Each estimation method ~~may differ~~differs in terms of ~~their~~-applicability, even within the
50 same area, because the different estimation methods include different physical and chemical soil properties (Lin
51 et al., 2017; Wang et al., 2013b; Kiani et al., 2016). Consequently, the estimated results can differ significantly
52 among methods because soil conditions vary by region (Lin et al., 2017; Wang et al., 2013b). Selecting the optimal
53 estimation method of soil erodibility is therefore critical to estimate the amount of soil erosion.

54 Soil erosion ~~in~~on the Loess Plateau of China is among the highest in the world (Fu et al., 2009; Huang et al.,
55 2016). The area affected by soil and water loss is as large as 4.5×10^5 km² (~71% of the local land area), and
56 the long-term average sediment loss is up to 1.6×10^9 t (Fu et al., 2017). To maintain water quality and ~~to~~ control
57 soil erosion (Fu et al., 2011), the Chinese government has implemented a large-scale policy to convert farmlands
58 to forests and grasslands since the 20th century (Lü et al., 2012; Feng et al., 2013b; Wu et al., 2016). Although
59 ~~this~~the large-scale introduction of vegetation ~~should reduce~~is expected to have reduced soil erosion, the extent of
60 the reduction remains unclear. ~~Accordingly~~Therefore, different estimation methods should be used to calculate
61 erosion factors, including the soil erodibility factor. In this ~~article~~study, the Ansai watershed ~~in~~of the Loess Plateau
62 of China was chosen as a case study, and the five above ~~five-mentioned~~ estimation methods of estimating K value
63 were ~~used, and the~~applied. The objectives of this study ~~are~~were (1) to estimate the soil erodibility factor with
64 different methods; (2) to select the ~~possible best texture-based~~optional method to estimate K ; and (3) to
65 understand ~~possible indirect environmental~~the influencing factors ~~on~~of soil erodibility for the local area.

66 2 Materials and methods

67 2.1 Study area

68 The Ansai watershed (108°5'44"-109°26'18"E, 36°30'45"-37°19'3"N) is located ~~in~~around the upper reaches
69 of the Yanhe River. in the inland hinterland of the northwestern Loess Plateau. This watershed lies in the northern
70 part of Shanxi ~~province~~Province and ~~the inland hinterland of the northwestern Loess Plateau and at the edge~~
71 ~~of~~borders the Ordos basin. It belongs to the typical loess hilly-gully region and covers an area of approximately
72 1334 km². The soil type in the study area is loess soil, with low fertility and high vulnerability to erosion (Zhao et
73 al., 2012; Yu et al., 2015).~~topography is complex and varied, and the ground surface is fragmented. The elevations~~
74 ~~within the watershed are high in the northwest and low in the southeast, and these elevations range from 997 to~~
75 ~~1731 m above sea level.~~ The topography is complex and varied, and the land surface is fragmented into different
76 land uses, dominated by~~The watershed belongs to the mid-temperate continental semi-arid monsoon climate region.~~
77 ~~The average annual precipitation is 505.3 mm, and 74 percent of the rainfall occurs from June to September. The~~
78 ~~predominant land-use types in the Ansai watershed are~~ rain-fed farmland, apple orchard, native grassland, pasture
79 grassland, shrubland, and forest (Feng et al., 2013a). The elevations within the watershed are high in the northwest
80 and low in the southeast, ranging between 997 and 1731 m above sea level. The watershed belongs to the mid-
81 temperate continental semi-arid monsoon climate region.~~The soil type in this study area is loess soil~~The average
82 annual precipitation is 505.3 mm, and 74% of the rainfall occurs from June to September. ~~with low fertility and~~
83 ~~high vulnerability to erosion (Zhao et al., 2012; Yu et al., 2015).~~

84 2.2 Sample point setting

85 The soil data used in this study came from 151 typical sample data sets that were obtained during soil surveys
86 conducted from July to September ~~in~~ 2014. The soil ~~type~~type of all 151 sample points ~~are~~is loess soil.
87 Representative vegetation types were selected, ~~which included:~~ (1) natural vegetation, ~~including:~~ native
88 ~~grassland~~grasslands (NG); (2) artificially managed vegetation types, ~~including:~~ apple orchards (AO) and farmland

89 (FL); and (3) artificially restored vegetation types, ~~including:~~ pasture ~~grassland~~grasslands (PG), sea buckthorn
90 (SB), *Caragana korshinskii* (CK), David's peach (DP), ~~and~~ and black locust (BL). The distance between each
91 vegetation ~~sampling site~~ sampling site was at least 2 km, and the area of each vegetation type was greater than 30 m by
92 30 m, ~~and the~~. The selected sample plots were distributed evenly within the study area. The sample plots within
93 the farmland and grassland had a size of 2 ~~m-by~~× 2 m, whereas the corresponding dimensions for the sample plots
94 within the shrubland and forest areas were 5 ~~m-by~~× 5 m and 10 ~~m-by~~× 10 m, respectively. Each sample plot was
95 ~~repeated~~replicated three times. The locations of the sampling points were determined using a GPS unit (Garmin
96 eTrex 309X), Garmin Ltd. subsidiary in Shanghai, China. The collected soil samples were taken ~~back~~ to the
97 laboratory, dried naturally, ground and ~~filtered~~sieved with a 2-mm sieve. The ~~grain~~soil particle size distributions
98 of the soil samples were evaluated using the hydrometer method. The size classes of ~~the~~soil particles in this study
99 were based on USDA classes and were as follows: sand (0.005-2.0 mm), silt (0.002-0.05 mm) and clay (< 0.002
100 mm) (Wang, et al., 2012).

101 To fully explore the primary factors influencing soil erodibility in the Ansai watershed, we chose four types
102 of environmental factors, ~~including:~~ physicochemical soil properties, topographic factors, climate factors and
103 vegetation factors. ~~While~~Although soil ~~erodibility~~erodibility does not directly depend on environmental factors,
104 soil properties such as soil particle size distribution and soil organic matter can be affected by environmental
105 factors. ~~Soil erodibility;~~ thus ~~has indirect relationship with the~~, environmental factors ~~have indirect relationships~~
106 with soil erodibility. These environmental factors covered 20 independent variables, ~~specifically:~~ elevation (Ele),
107 slope position (SP), slope aspect (SA), slope gradient (SG), slope shape (SS), clay ~~(Cla)~~ content, (Cla), silt ~~(Sil)~~
108 content, (Sil), sand ~~(San)~~ content, (San), organic matter (OM) content, soil bulk density (SBD), porosity (Por),
109 average annual rainfall (AAR), vegetation coverage (VC), aboveground biomass (AB), vegetation height (VH),
110 litter biomass (LB), plant density (PD), crown width (Cro), basal diameter (BD), and branch number (BN). All of

111 the data on environmental factors were derived from the field surveys. The main characteristics and sampling
 112 numbers for the study area are shown in Table 1, and the sampling points are shown in Fig. 1. Based on the results
 113 of the Spearman correlation analysis, we ~~then~~ retained some environmental variables that displayed significant
 114 correlations ($P < 0.05$) with soil erodibility to perform a principal component analysis (PCA) and ~~to~~ obtain the
 115 minimum data set (MDS) (Xu et al., 2008). Only those principal components (PCs) with eigenvalues $N > 1.0$ and
 116 only those variables with highly weighted factor loadings (i.e., those with absolute values within 10% of the highest
 117 value) were retained for the MDS (Mandal et al., 2008).

118 2.3 Research methods

119 Soil erodibility indicates the degree of difficulty ~~thatwith which~~ soil becomes separated, eroded and
 120 transported by rainfall ~~erosionerosivity~~ (Wang et al., 2013a; Cerdà et al., 2017). ~~Soil~~The soil erodibility factor,
 121 which is commonly known as the K -factor in ~~the model~~models, is defined as the average rate of soil loss per unit
 122 of rainfall erosivity index from a cultivated continuous fallow plot on a 22.1-m-long, 9% slope in the universal
 123 soil loss equation (Zhang et al., 2008). To minimize bias from ~~using only oneany single~~ estimation method, we
 124 estimated the K values using five estimation models (i.e., EPIC, NOMO, M-NOMO, Torri and Shirazi), ~~thatwhich~~
 125 have been widely applied in ~~the~~ research on soil erodibility (Wischmeier et al., 1971, 1978; Williams et al., 1990;
 126 Torri et al., 1997; Shirazi et al., 1988).

127 2.3.1 K value estimation using the EPIC model

128 The erosion-productivity impact model (EPIC) developed by Williams (Williams et al. 1990) is as follows:

$$\begin{aligned}
 K &= \left[0.2 + 0.3e^{-0.0256.SAN\left(1-\frac{SIL}{100}\right)} \right] \left(\frac{SIL}{CLA + SIL} \right)^{0.3} \left(1.0 - \frac{0.25C}{C + e^{3.72 - 2.95C}} \right) \left(1.0 - \frac{0.7SN_1}{SN_1 + e^{-5.51 + 22.9SN_1}} \right) \\
 K &= \left[0.2 + 0.3e^{-0.0256.SAN\left(1-\frac{SIL}{100}\right)} \right] \left(\frac{SIL}{CLA + SIL} \right)^{0.3} \left(1.0 - \frac{0.25C}{C + e^{3.72 - 2.95C}} \right) \left(1.0 - \frac{0.7SN_1}{SN_1 + e^{-5.51 + 22.9SN_1}} \right)
 \end{aligned}
 \tag{1}$$

129 where SAN is ~~the~~ percent sand content, SIL is ~~the~~ percent silt content, CLA is ~~the~~ percent clay content, C is ~~the~~

130 percent organic carbon content, and $SN_1 = 1 - \frac{SAN}{100}$. The resulting K value is reported in United States
131 customary units of [short ton·ac·h / (100 ft·short ton·ac·in)].

132 2.3.2 K value estimation using the NOMO model

133 Wischmeier (Wischmeier et al., 1971) proposed this model after analyzing the ~~relationship~~relationships
134 between soil erosion and five soil characteristic indicators, ~~including the~~: percent silt+ + very fine sand fraction
135 (0.05-0.1 mm), ~~the~~ percent sand fraction, ~~the~~ soil organic matter content, a code for soil structure, and a code for
136 soil permeability:

$$\begin{aligned} \cancel{K} &= [2.1 \times 10^{-4} M^{1.14} (12 - OM) + 3.25(S - 2) + 2.5(P - 3)] / 100 \\ K &= [2.1 \times 10^{-4} M^{1.14} (12 - OM) + 3.25(S - 2) + 2.5(P - 3)] / 100 \end{aligned} \quad (2)$$

137 where M is the product of the percent of silt+ + very fine sand and the percent of all soil fractions other than clay,
138 OM is ~~the~~ soil organic matter content (%), S is ~~the~~ soil structure code, and P is ~~the~~ soil permeability code. The
139 resulting K value is reported in United States customary units of [short ton·ac·h ~~h~~ / (100 ft·short ton·ac·in)].

140 2.3.3 K value estimation using the M-NOMO model

141 On the basis of the universal soil loss equation (USLE) model, the RUSLE model was modified for calculating
142 soil erodibility; ~~that is, a~~the revised nomograph equation was ~~devised~~modified from the previous nomograph
143 equation (Wischmeier et al., 1978) ~~based on the nomograph equation~~. The revised nomograph equation is as
144 follows:

$$\begin{aligned} \cancel{K} &= [2.1 \times 10^{-4} M^{1.14} (12 - OM) + 3.25(2 - S) + 2.5(P - 3)] / 100 \\ K &= [2.1 \times 10^{-4} M^{1.14} (12 - OM) + 3.25(2 - S) + 2.5(P - 3)] / 100 \end{aligned} \quad (3)$$

145 where M is the product of the percent of silt+ + very fine sand and the percent of all soil fractions other than clay,
146 OM is ~~the~~ soil organic matter content (%), S is ~~the~~ soil structure code, and P is ~~the~~ soil permeability code. The
147 resulting K value is reported in United States customary units of [short ton·ac·h ~~h~~ / (100 ft·short ton·ac·in)].

148 2.3.4 *K* value estimation using the Torri model

149 Torri (Torri et al., 1997) established this model in 1997 using data describing soil particle size and soil organic
 150 matter content. The model has few parameters; and simple data acquisition of the relevant data is simple. The
 151 formula used in evaluating for this model is as follows:

$$\begin{aligned}
 & \cancel{K = 0.0293(0.65 - D_g + 0.24D_g^2) \times \exp\left\{-0.0021 \frac{OM}{c} - 0.00037 \left(\frac{OM}{c}\right)^2 - 4.02c + 1.72c^2\right\}} \\
 & K = 0.0293(0.65 - D_g + 0.24D_g^2) \times \exp\left\{-0.0021 \frac{OM}{c} - 0.00037 \left(\frac{OM}{c}\right)^2 - 4.02c + 1.72c^2\right\}
 \end{aligned} \tag{4}$$

152 where OM is the and c are percent content of soil organic matter; and e is the percent content of clay. In addition,
 153 the content, respectively. D_g can be calculated by using the following formula:

$$\cancel{D_g = \sum f_i \lg \sqrt{d_i d_{i-1}}} \quad D_g = \sum f_i \lg \sqrt{d_i d_{i-1}} \tag{5}$$

154 where D_g is the Napierian logarithm of the geometric mean of the particle size distribution, d_i (mm) is the maximum
 155 diameter of the i -th class, d_{i-1} (mm) is the minimum diameter and f_i is the mass fraction of the corresponding
 156 particle size class. We calculate the calculated D_g based on three particle-size classes, namely: sand, silt, and clay.
 157 The resulting K values are reported in the international units of [(t·hm²·h)~~(t)~~ / (MJ·mm·hm²)].

158 2.3.5 *K* value estimation using the Shirazi model

159 Shirazi (Shirazi et al., 1988) put forward a model that is appropriate for situations involving fewer few physical
 160 and chemical properties of the soil materials. He The authors suggested that K values can be calculated through
 161 considering by using only the geometric mean diameter (D_g) of the soil grains. The relevant formula is:

$$\cancel{K = 7.594 \left\{ 0.0034 + 0.0405 e^{-\frac{1}{2} \left[\frac{\log(D_g) + 1.659}{0.7101} \right]^2} \right\}} \quad K = 7.594 \left\{ 0.0034 + 0.0405 e^{-\frac{1}{2} \left[\frac{\log(D_g) + 1.659}{0.7101} \right]^2} \right\} \tag{6}$$

$$\cancel{D_g (mm) = e^{0.01 \sum f_i \ln m_i}} \quad \text{Meanwhile, } D_g \text{ in this model can be calculated by using the following} \tag{7}$$

formula:

$$D_g (mm) = e^{0.01 \sum f_i \ln m_i}$$

162 where D_g is the geometric mean diameter of the soil particles, where f_i is the weight percentage of the i -th particle
 163 size fraction (%), m_i is the arithmetic mean of the particle size limits for the i -th fraction (mm), and n is the number
 164 of particle size fractions. The resulting K value is reported in United States customary units of [short ton·ac·h^{1/2}
 165 (100 ft·short ton·ac·in)].

166 2.3.6 K value comparisons

167 To increase the comparability of the results from the different estimation models, our research adopted the
 168 international units for the K values, [t·hm²·hr^{1/2}/(MJ·mm·hm²)]. The international K value is equal to the K value
 169 reported in the United States customary units multiplied by 0.1317. To clarify the form of the distribution, we
 170 collected the frequency distribution figures of soil erodibility for each model (Wei et al., 2017a, b). The K values
 171 obtained using the five methods were normally distributed ($P > 0.05$). Therefore, the soil erodibility K values
 172 measured within the study area were statistically analyzed directly, without the need for data conversion (Fang et
 173 al., 2016)., multiplied by 0.1317. To discuss the possible best texture-based method to estimate K , related research
 174 on K estimation, especially that involving measured values of K on the Loess Plateau of China, was consulted. A
 175 Taylor diagram was also used to compare the models.

176 To clarify the form of the distribution, we adopted the Kolmogorov-Smirnov test (Table 2) and made the
 177 frequency distribution figures of soil erodibility for each model (Fig. 2). The $P > 0.05$ showed that the K values
 178 obtained using the five methods were normally distributed. Therefore, the soil erodibility K values measured within
 179 the study area can be analyzed directly using statistical methods without data conversion (Fang et al. 2016).

180 ~~2.3.6 K value comparisons~~

181 In order to discuss the possible best texture-based method to estimate K , related researches on K estimation,
 182 especially the measured value of K in Loess Plateau of China, have been collected. Taylor Diagram was also used

183 ~~to compare the difference between models.~~

184 3 Results

185 3.1 Soil erodibility in the Ansai watershed based on five different models ~~in Ansai watershed~~

186 We ~~found that the obtained different values when calculating~~ descriptive statistics of the ~~K values~~ value in the
187 Ansai watershed ~~differed when among the~~ different models ~~were used~~ (Table 2). The range of K values based on
188 the five methods were between 0.032 and 0.060, 0.046 and 0.092, 0.047 and 0.088, 0.009 and 0.066, and 0.018
189 and 0.044 [$t \cdot \text{hm}^2 \cdot \text{hr} / (\text{MJ} \cdot \text{mm} \cdot \text{hm}^2)$] for K_{EPIC} , K_{NOMO} , $K_{\text{M-NOMO}}$, K_{Torri} , and K_{Shirazi} , respectively. The ~~range of the~~
190 maximum values were 1.875, 2.000, 1.872, 7.333 and 2.444 times larger than the corresponding minimum values
191 (Table 2). The differences between the mean and median values were 0.001, -0.001, 0.000, 0.000, and 0.000
192 [$t \cdot \text{hm}^2 \cdot \text{hr} / (\text{MJ} \cdot \text{mm} \cdot \text{hm}^2)$] for K_{EPIC} , K_{NOMO} , $K_{\text{M-NOMO}}$, K_{Torri} , and K_{Shirazi} , respectively. The standard deviations
193 (SDs) of the K values were 0.408, -0.447, -1.079, -2.639, and 0.059 ~~for K_{EPIC} , K_{NOMO} , $K_{\text{M-NOMO}}$, K_{Torri} , and K_{Shirazi} ,~~
194 respectively, ~~and the skewnesses.~~ The skewness values of the K values were 0.946, 0.956, 4.353, 16.872, and
195 0.009 ~~for K_{EPIC} , K_{NOMO} , $K_{\text{M-NOMO}}$, K_{Torri} , and K_{Shirazi} ,~~ respectively. The C_v value of $K_{\text{M-NOMO}}$ was $0.067 < 10\%$;
196 ~~in addition,%, and~~ the C_v values of K_{EPIC} , K_{NOMO} , K_{Torri} , and K_{Shirazi} were 0.109, 0.110, 0.113, and 0.182, respectively,
197 all of which ~~were corresponded to~~ between 10% and 100%.

198 In the Taylor diagrams (Taylor, 2001) (Fig. 32), the K values based on the EPIC model ~~is were~~ used as the
199 reference ~~objectobjects~~. The K values based on the Torri, NOMO, and Shirazi models were similar and ~~were~~
200 located close to each other. In contrast, ~~there was inconsistency in~~ the K values estimated by the M-NOMO and
201 EPIC models ~~were inconsistent with the other K values~~.

202 3.2 Spearman correlation coefficients ~~betweenof~~ soil erodibility and environmental variables in the Ansai 203 watershed

204 The correlations between soil erodibility and the environmental variables varied ~~withamong~~ the different

205 vegetation types (Table S1-S4). In general, soil erodibility in artificially managed vegetation types (apple orchards
206 and David's peach) and artificially restored vegetation types (e.g., sea buckthorn and black locust) had significant
207 ~~correlation~~correlations with vegetation properties. For example, soil erodibility in areas planted with apple
208 orchards had a significant positive correlation with plant density ($P < 0.05$, Table S1). ~~The soil~~Soil erodibility ~~of in~~
209 areas with sea buckthorn had significant negative correlations with ~~the~~ slope gradient and plant density, ~~whereas~~
210 ~~it had~~ and significant positive correlations with ~~the~~ average annual rainfall and aboveground biomass ($P < 0.05$,
211 Table S3). ~~The soil~~Soil erodibility of areas with David's peach had ~~a~~ significant positive correlation with ~~the~~
212 aboveground biomass, ~~whereas it had~~ and significant negative correlations with ~~the~~ slope gradient, vegetation
213 coverage, vegetation height, crown width and basal diameter ($P < 0.05$, Table S4). ~~The soil~~Soil erodibility ~~of in~~
214 areas with black locust had ~~a~~ significant negative correlation with ~~the~~ elevation, ~~whereas it had~~ and significant
215 positive correlations with ~~the~~ slope position, slope gradient, soil bulk density, vegetation coverage, litter biomass
216 and branch number ($P < 0.05$, Table S4). ~~Meanwhile, soil~~Soil erodibility in areas under ~~different~~other vegetation
217 types, such as ~~grasslands~~grassland or ~~farmlands were~~farmland, was more strongly correlated with soil or landscape
218 properties. than other impact factors. The results of the ~~correlation analysis~~analyses of correlations between
219 estimated K values and the selected environmental variables showed that soil erodibility in farmlands had
220 significant positive correlations with ~~the slope position~~, slope shape and ~~average annual rainfall and displayed a~~
221 significant negative correlation with ~~the~~ slope gradient ($P < 0.05$, Table S1). ~~Soil~~The soil erodibility of areas with
222 native grasslands had ~~a~~ significant a negative correlation with ~~the~~ elevation, ~~whereas it had~~ and significant
223 positive correlations with ~~the~~ average annual rainfall and slope gradient ($P < 0.05$, Table S2). ~~Soil~~The soil
224 erodibility of areas with pasture grasslands did not have significant correlations with ~~the~~ environmental variables
225 other than soil organic matter content and ~~the~~ soil particle size ($P < 0.05$, Table S2). ~~The soil~~Soil erodibility ~~of in~~
226 areas with *Caragana korshinskii* had a significant positive correlation with ~~the~~ elevation, ~~whereas it had~~ and a

227 significant negative correlation with ~~the~~ average annual rainfall ($P < 0.05$, Table S3).

228 3.3 Principal component analysis of soil erodibility under different vegetation types

229 ~~Our results showed the~~The PCA identified one PC each for apple orchards, native grasslands, sea buckthorn,
230 *Caragana korshinskii* and pasture grasslands, which accounted for 100%, 48.88%, 62.05% and 53.61 of the
231 variances, respectively (Table S5). ~~The PCA identified two PCs each for farmland and David's peach; the~~
232 ~~corresponding cumulative variances were 73.93 % and 81.07 %, respectively.~~ For black locust, the PCA identified
233 ~~three PCs that accounted for 70.25 % of the variance (Table S5). In farmland, PC1 included two variables that had~~
234 ~~highly weighted factor loadings, the slope shape and slope position, and PC2 included only the slope gradient,~~
235 ~~which had a highly weighted factor loading. In apple orchards, the highly weighted factor loading was the plant~~
236 ~~density. In was the primary contributor to the high factor loading.~~ For native grasslands, PC1 included two
237 variables that had highly weighted factor loadings, ~~including~~ the slope gradient and elevation. ~~The pasture~~Pasture
238 grasslands had no variables with ~~highly weighted~~high factor loadings because it had no significant environmental
239 variables except ~~the~~ soil particle size and soil organic matter. The highly weighted factor loadings in areas with
240 sea buckthorn were ~~the~~ slope gradient, aboveground biomass and plant density. In areas planted with *Caragana*
241 *korshinskii*, two variables had ~~highly weighted factor loadings, including the average annual rainfall and elevation.~~
242 ~~In areas planted with black locust, the highly weighted factor loadings of PC1 were the slope position, elevation~~
243 ~~and litter biomass; for PC2, the slope gradient and soil bulk density had high factor loadings, whereas only~~
244 ~~vegetation coverage had a high weighted factor loading for PC3. In areas planted with David's peach, PC1 included~~
245 ~~three variables that had highly weighted factor loadings, specifically the crown width, vegetation height and~~
246 ~~vegetation coverage, whereas only the basal diameter had a high factor loading for PC2~~high factor loadings:
247 average annual rainfall and elevation (Table S5).

248 The PCA identified two PCs each for farmland and David's peach; the corresponding cumulative variances

249 were 73.93% and 81.07%, respectively. The PC1 for farmland included two variables that had high factor loadings,
250 slope shape and slope position, whereas PC2 only included slope gradient. In areas planted with David's peach,
251 crown width, vegetation height and vegetation coverage contributed to the high factor loading of PC1, whereas
252 basal diameter alone had a high factor loading for PC2. In areas planted with black locust, the PCA identified three
253 PCs that accounted for 70.25% of the variance (Table S5). PC1 had slope position, elevation and litter biomass as
254 parameters with high factor loadings. The parameters with high factor loadings for PC2 were slope gradient and
255 soil bulk density, and vegetation coverage had a high factor loading for PC3 (Table S5).

256 The MDS of ~~the~~ soil erodibility included six environmental variables for black locust, four for David's peach,
257 three each for farmland and sea buckthorn, two each for native grasslands and *Caragana korshinskii*, one for apple
258 orchards and none for pasture grasslands (Table ~~3~~S1, Table S2, Table S3). In addition to ~~the~~ soil organic matter
259 and soil particle size, which ~~are~~were included in the *K* value estimation equations, the dominant factors affecting
260 ~~the~~ soil erodibility for farmland were slope shape, slope gradient and slope position. For apple orchards, the only
261 dominant factor affecting soil erodibility (~~except the~~other than soil organic matter and soil particle size) was plant
262 density. For areas with native grasslands, the dominant factors affecting soil erodibility were soil organic matter,
263 soil particle size, slope gradient and elevation. For areas with sea buckthorn, the dominant factors affecting soil
264 erodibility were aboveground biomass, slope gradient and plant density in addition to the two soil properties. The
265 dominant factors affecting soil erodibility in areas with *Caragana korshinskii* were soil particle size, soil organic
266 matter, average annual rainfall and elevation. For areas with black locust, the dominant factors were ~~the~~ slope
267 gradient, slope position, elevation, litter biomass, soil bulk density and vegetation coverage in addition to the soil
268 organic matter and soil particle size. The dominant factors affecting soil erodibility in areas with David's peach
269 included ~~the~~ soil organic matter, soil particle size, crown width, vegetation height and vegetation coverage.

270 **4 Discussion**

271 4.1 The optimal methods for estimating K values in the Ansai watershed

272 In this study, we found that different models resulted in different ~~estimations~~estimates of soil erodibility
273 (Table 2). Since the different estimation methods use different soil attributes as input parameters; ~~even if the input~~
274 ~~parameters are the same~~, the decision coefficients of the same input parameters ~~are different~~will differ. For
275 example, the EPIC model focuses on the features of the soil ~~partiele~~particles and soil nutrients, ~~while~~whereas the
276 NOMO model focuses on not only ~~the~~ soil particle size and soil nutrient characteristics; but also the soil
277 ~~structure~~structural characteristics, such as soil structure code and soil permeability code. The existing soil
278 erodibility estimation equations are used to calculate soil erodibility based on data on ~~the~~ physicochemical soil
279 properties, such as soil texture, soil structure, soil permeability and soil organic matter content (Wischmeier et al.,
280 1971, 1978; Williams et al., 1990; Torri et al., 1997; Shirazi et al., 1988). Among these factors, the main physical
281 soil property is ~~the~~ soil particle composition, such as the contents of sand, silt and clay, and the main chemical soil
282 property is ~~the~~ soil organic matter content (Wei et al., 2017).

283 Our results showed that the K values based on the Torri, NOMO, and Shirazi models were ~~are~~ located close
284 to each other in the Taylor diagrams (Fig. ~~3~~ 2) and ~~those that these~~ three models could therefore represent ~~the~~ soil
285 erodibility in the Ansai watershed. Based on previous studies, these models have ~~also~~ been recommended as the
286 optimal models ~~in Chinese for China's~~ subtropical zone, China's purple hilly region, Northeast China, and ~~Chinese~~
287 ~~Loess~~China's Loess Plateau (Table 4). ~~We, however, suggested~~ However, we suggest that the Torri and Shirazi
288 models ~~as better representatives of~~ are the best models; based on ~~their~~ estimated K values ~~and the~~ derived from these
289 models and actual (measured) soil erodibility data ~~in from the~~ Ansai watershed (Zhang et al., 2001; Table S6). The
290 estimated K ~~value~~values based on the Torri and Shirazi models were closer to the measured soil erodibility data
291 among those of the three possible appropriate models (Table 2 and Table S6). Our ~~suggestions were also~~ findings
292 are supported by a study by Lin et al. (2017) ~~who showed~~ showing that the estimated K ~~value~~values based on the

293 Torri and Shirazi models ~~was~~were closer to the measured value- than NOMO model and M-NOMO model.

294 4.2 Environmental factors that influenced ~~the~~ soil erodibility

295 Based on the definition of K factor by Wischmeier et al. (1971), soil ~~erodibility~~erodibility is estimated ~~by~~from
296 texture data, organic matter content, soil structure index, and the soil permeability index. While soil
297 ~~erodibility~~erodibility does not directly depend on environmental factors, soil properties such as soil particle size
298 distribution and soil organic matter can be affected by environmental factors. Soil erodibility thus has indirect
299 ~~relationship~~relationships with ~~the~~ environmental factors, particularly vegetation type ~~that, which~~ influences the
300 generation of soil organic matter and the composition of soil ~~partiele~~particles. Soil erodibility had ~~different~~
301 ~~correlation~~various correlations with the selected environmental variables, which ~~resulted in changes in~~affected the
302 dominant factors ~~that influenced the~~influencing soil erodibility (Tables S1-S5, Table 3). In native grasslands, soil
303 erodibility had significant correlations with terrain factors (e.g., elevation, slope degree) (Table S1, Table S4), and
304 the dominant factors influencing ~~the~~ soil erodibility were soil properties and topography. Terrain factors have close
305 relationships with soil properties. With ~~the increase~~changes of elevation and slope, the physical and chemical ~~soil~~
306 properties of soil (e.g., soil permeability, soil bulk density, and soil ~~nutrient~~nutrients) and soil surface conditions
307 ~~are changed, further lead~~(e.g., roughness, litter layer) change, leading to ~~the~~ changes ~~of~~in soil particle size
308 composition and soil erodibility (Zhao et al., 2015). For example, Li et al. (2011) found that the silt content was
309 higher than the sand content in low ~~than~~but not high elevations, and Liu et al. (2005) found that slope gradient
310 ~~is~~was negatively correlated with soil nutrients (e.g., soil organic matter, available nitrogen).

311 For most artificially managed vegetation types (apple orchards and David's peach) and artificially restored
312 vegetation types (e.g., sea buckthorn and black locust), soil erodibility had significant correlations with ~~the~~
313 vegetation properties (Table S1, Table S3-S4). By ~~changing the~~affecting physicochemical soil properties and soil
314 structure stability, vegetation properties ~~could~~ affect soil erodibility. For example, the dominant ~~factor(s)~~factors

315 influencing ~~the~~ soil erodibility ~~associated with~~ were plant density for apple orchards ~~was plant density, sea~~
316 ~~buckthorn was,~~ aboveground biomass, ~~black locust were~~ for sea buckthorn litter biomass and vegetation
317 coverage for black locust, and ~~David's peach were~~ crown width, vegetation height, basal diameter and vegetation
318 coverage for David's peach (Table S1). ~~Because all these vegetation types are more or less affected by~~
319 ~~human~~ Human activities, ~~soil erodibility can also indirectly be affected by~~ (e.g., pruning) affect vegetation recovery
320 and land cover change. These changes may then influence vegetation properties and thereby impact soil erodibility.

321 5 Conclusions

322 We evaluated soil erodibility in the Ansai watershed using five estimation models ~~in Ansai watershed; the~~
323 The estimated K values ~~based on~~ differed among the different models ~~were different from one another and the~~
324 ~~resulting K values~~ ranged between 0.009 and 0.092 t·hm²·hr⁻¹ / (MJ·mm·hm²). Based on Taylor diagrams and
325 previous studies, we considered the Shirazi and Torri ~~model~~ models the optimal models for the Ansai watershed.
326 Since soil erodibility is estimated by soil properties, ~~soil erodibility~~ it has indirect ~~relationship~~ relationships with
327 ~~environment~~ environmental factors, including elevation and slope degree, and, to a lesser extent, human activities.
328 By changing vegetation density, biomass, and cover, ~~human~~ humans can indirectly affect soil erodibility.

329 **Acknowledgments** This work was supported by the National Key Research Program of China (No.
330 2016YFC0501604), the National Natural Science Foundation of China (No. 41771197), and the State Key
331 Laboratory of Earth Surface Processes and Resource Ecology (No. 2017-FX-01(2)). We would like to thank Jing
332 Wang, Xiao Zhang, Qiang Feng, Xuening Fang, Jingyi Ding, and Yuanxin Liu for their support and contributions
333 during the fieldwork.

334 References

335 Bagarello, V., Stefano, C. D., Ferro, V., Giordano, G., Iovino, M., Pampalone, V.: Estimating the USLE soil
336 erodibility factor in Sicily, south Italy, Appl. Eng. Agric., 28, 199–206, 2012.

337 Bonilla, C. A., Johnson, O. I.: Soil erodibility mapping and its correlation with soil properties in Central Chile,
338 Geoderma, 189–190, 116–123, 2012.

339 Bryan, R. B., Govers, G., Poesenb, S. R. A.: The concept of soil erodibility and some problems of assessment and
340 application, Catena, 16, 393–412, 1989.

341 Cerdà, A., Keesstra, S. D., Rodrigo-Comino, J., Novara, A., Pereira, P., Brevik, E., Gimenez-morera A, Fernandez-
342 raga M, Pulido M, Prima S D, Jordán, A.: Runoff initiation, soil detachment and connectivity are enhanced
343 as a consequence of vineyards plantations, J. Environ. Manage., 202, 268–275, 2017.

344 Cerdà, A.: Soil aggregate stability under different Mediterranean vegetation types, Catena, 32, 73–86, 1998.

345 Chen, X. Y., Zhou, J.: Volume-based soil particle fractal relation with soil erodibility in a small watershed of
346 purple soil, Environ. Earth Sci., 70, 1735–1746, 2013.

347 Fang, X. N., Zhao, W. W., Wang, L. X., Feng, Q., Ding, J. Y., Liu, Y. X., Zhang, X.: Variations of deep soil moisture
348 under different vegetation types and influencing factors in a watershed of the Loess Plateau, China, Hydrol.
349 Earth Syst. Sci., 20, 3309–3323, 2016.

350 Feng, Q., Zhao, W. W., Qiu, Y., Zhao, M. Y., Zhong, L. N.: Spatial heterogeneity of soil moisture and the scale
351 variability of its influencing factors: a case study in the Loess Plateau of China, Water, 5, 1226–1242, 2013a.

352 Feng, X. M., Fu, B. J., Lu, N., Zeng, Y., Wu, B. F.: How ecological restoration alters ecosystem services: an
353 analysis of carbon sequestration in China's Loess Plateau, Sci. Rep-UK., 3, 28–46, 2013b.

354 Ferreira, V., Panagopoulos, T., Andrade, R., Guerrero, C., Loures, L.: Spatial variability of soil properties and soil
355 erodibility in the Alqueva reservoir watershed, Solid Earth, 6, 383–392, 2015.

356 Fu, B. J., Liu, Y., Lü, Y. H., He, C. S., Zeng, Y., Wu, B. F.: Assessing the soil erosion control service of ecosystems
357 change in the Loess Plateau of China, Ecol. Complex., 8, 284–293, 2011.

358 Fu, B. J., Wang, S., Liu, Y., Liu, J. B., Liang, W., Miao, C. Y.: Hydrogeomorphic ecosystem responses to natural
359 and anthropogenic changes in the Loess Plateau of China, *Annu. Rev. Earth Planet Sci.*, 45, 223–243, 2017.

360 Fu, B. J., Wang, Y. F., Lü, Y. H., He, C. S., Chen, L. D., Song, C. J.: The effects of land use combination on soil
361 erosion-a case study in Loess Plateau of China, *Prog. Phys. Geog.*, 33, 793–804, 2009.

362 Fu, B. J., Zhao, W. W., Chen, L. D., Zhang, Q. J., Lü, Y. H., Gulinck, H., Poesen, J.: Assessment of soil erosion at
363 large watershed scale using RUSLE and GIS: a case study in the Loess plateau of China, *Land Degrad. Dev.*,
364 16, 73–85, 2005.

365 Huang, J., Wang, J., Zhao, X. N., Li, H. B., Jing, Z. L., Gao, X. D., Chen, X. L., Pute, W.: Simulation study of the
366 impact of permanent groundcover on soil and water changes in jujube orchards on sloping ground, *Land
367 Degrad. Dev.*, 27(4), 946–954, 2016.

368 Hussein, M. H.: A sheet erodibility parameter for water erosion modeling in regions with low intensity rain,
369 *Hydrol. Res.*, 44, 1013–1021, 2013.

370 Igwe, C. A.: Erodibility of soils of the upper rainforest zone, southeastern nigeria, *Land Degrad. Dev.*, 14, 323–
371 334, 2003.

372 Kiani, F., Ghezelseflo, A.: Evaluation of soil erodibility factor(k) for loess derived landforms of Kechik
373 watershed in Golestan Province, North of Iran, *J. Mt. Sci-Engl.*, 13, 2028–2035, 2016.

374 Li, P., Li, Z. B., Zheng, Y.: Effect of different elevation on soil physical-chemical properties and erodibility in
375 dry-hot valley, *Bull. Soil Water Conserv.*, 31, 103–107, 2011. (in Chinese with English abstract).

376 Lin, F., Zhu, Z. L., Zeng, Q. C., An, S. S.: Comparative study of three different methods for estimation of soil
377 erodibility K in Yanhe Watershed of China, *Acta Pedologi Sinica.*, 54(5), 1136–1146, 2017. (in Chinese with
378 English abstract).

379 Liu, S. L., Guo, X. D., Lian, G., Fu, B. J., Wang, J.: Multi-scale analysis of spatial variation of soil characteristics
380 in Loess Plateau-case study of Hengshan County, *J. Soil Water Conserv.*, 19, 105–108, 2005. (in Chinese with
381 English abstract).

382 Lü, Y. H., Fu B.J., Feng X. M., Zeng, Y., Liu, Y., Chang, R. Y., Sun, G., Wu, B. F.: A policy-driven large scale
383 ecological restoration: quantifying ecosystem services changes in the Loess Plateau of China, *PLoS ONE*, 7,
384 17–28, 2012.

385 Mandal, U. K., Warrington, D. N., Bhardwaj, A. K., Bar-Tal, A., Kautsky, L., Minz, D., Levy, G. J.: Evaluating
386 impact of irrigation water quality on a calcareous clay soil using principal component analysis, *Geoderma*,
387 144, 189–197, 2008.

388 Mwaniki, M. W., Agutu, N. O., Mbaka, J. G., Ngigi, T. G., Waithaka, E. H.: Landslide scar/soil erodibility mapping
389 using Landsat TM/ETM+ bands 7 and 3 normalised difference index: A case study of central region of
390 Kenya, *Appl Geogr.*, 64, 108–120, 2015.

391 Wang, D. C., Zhang, G. L., Pan, X. Z., Zhao, Y. G., Zhao, M. S., Wang, G. F.: Mapping soil texture of a plain area
392 using fuzzy-c-means clustering method based on land surface diurnal temperature difference, *Pedosphere*, 22,
393 394-403, 2012.

394 Parajuli, S. P., Yang, Z., Kocurek, G.: Mapping erodibility in dust source regions based on geomorphology,
395 meteorology, and remote sensing, *J. Geophys. Res. Earth Surf.*, 119, 1977–1994, 2015.

396 Sanchis, M. P. S., Torri, D., Borselli, L., Poesen, J.: Climate effects on soil erodibility, *Earth Surf. Proc. Land*, 33,
397 1082–1097, 2012.

398 Sepúlveda-Lozada, A., Geissen, V., Ochoa-Gaona, S., Jarquin-Sanchez, A., dela-Cruz, S. H., Capetillo, E.,
399 Zamora- Cornelio, L. F., Revista, D. B. T.: Influence of three types of riparian vegetation on fluvial erosion
400 control in Pantanos de Centla, Mexico, *Rev. Biol. Trop.*, 57, 1153–1163, 2009.

401 Shirazi, M. A., Hart, J. W., Boersma, L.: A unifying quantitative analysis of soil texture: improvement of precision
402 and extension of scale, *Soil Sci. Soc. of Am. J.*, 52, 181–190, 1988.

403 Tang, F. K., Cui, M., Lu, Q., Liu, Y. G., Guo, H. Y., Zhou, J. X.: Effects of vegetation restoration on the aggregate
404 stability and distribution of aggregate-associated organic carbon in a typical karst gorge region, *Solid Earth*,
405 7, 141–151, 2016.

406 Taylor, K.: Summarizing multiple aspects of model performance in a single diagram, *J. Geophys. Res.*, 106, 7183–
407 7192, 2001.

408 Torri, D., Poesen, J., Borselli, L.: Predictability and uncertainty of the soil erodibility factor using a global
409 dataset, *Catena*, 31, 1–22, 1997.

410 Vaezi, A. R., Abbasi, M., Bussi, G., Keesstra, S.: Modeling sediment yield in semi-arid pasture Micro Catchments,
411 NW Iran, *Land Degrad. Dev.*, 28, 1274–1286, 2016b.

412 Vaezi, A. R., Hasanzadeh, H., Cerda, A.: Developing an erodibility triangle for soil textures in semi-arid regions,
413 NW Iran, *Catena*, 142, 221–232, 2016a.

414 Wang, A. J., Li, Z. G.: Spatial distribution of soil erodibility in Upper Yangtze River Region, *Adv. Mater Res.*, 610–
415 613, 2944–2947, 2012.

416 Wang, B., Zheng, F. L., Römken, M. J. M., Darboux, F.: Soil erodibility for water erosion: A perspective and
417 Chinese experiences, *Geomorphology*, 187, 1–10, 2013a.

418 Wang, B., Zheng, F. L., Römken, M. J. M.: Comparison of soil erodibility factors in USLE, RUSLE2, EPIC
419 and Dg models based on a Chinese soil erodibility database, *Acta Agr. Scand. B-S. P.*, 63, 69–79, 2013b.

420 Wang, G. Q., Fang, Q. F., Wu, B. B., Yang, H. C., Xu, Z. X.: Relationship between soil erodibility and modeled
421 infiltration rate in different soils, *J. Hydrol.*, 528, 408–418, 2015.

422 Wei, H., Zhao, W. W., Wang, J.: Research process on soil erodibility, *Chin. J. Appl. Ecol.*, 28, 2749–2759, [2017](#).
423 [2017a.](#) (in Chinese with English abstract).

424 [Wei, H., Zhao, W. W., Wang, J.: The optimal estimation method for K value of soil erodibility: A case study in](#)
425 [Ansai Watershed, *Science of Soil and Water Conservation*, 15, 52-62, 2017b.](#) (in Chinese with English
426 abstract).

427 Williams, J. R.: The erosion-productivity impact calculator (EPIC) model: A case history, *Phil. Trans. R. Soc. B.*,
428 329, 421–428, 1990.

429 Wischmeier, W. H., Johnson, C. B., Cross, B. V.: Soil erodibility nomograph for farmland and construction
430 sites, *J. Soil Water Conserv.*, 26, 189–193, 1971.

431 Wischmeier, W. H., Smith, D. D.: Predicting rainfall erosion losses-a guide to conservation planning, United
432 States. Dept. of Agriculture Handbook, 537, 1978.

433 Wu, L., Liu, X., Ma, X.: Application of a modified distributed-dynamic erosion and sediment yield model in a
434 typical watershed of hilly and gully region, Chinese Loess Plateau, *Solid Earth*, 1–26, 2016.

435 Xu, X. L., Ma, K. M., Fu, B. J., Song, C. J., Liu, W.: Relationships between vegetation and soil and topography in
436 a dry warm river valley, SW China, *Catena*, 75, 138–145, 2008.

437 Yu, Y., Wei, W., Chen, L. D., Yang, L., Jia, F. Y., Zhang, H. D.: Responses of vertical soil moisture to rainfall pulses
438 and land uses in a typical loess hilly area, china, *Solid Earth*, 6(2), 595–608, 2015.

439 Zhang, K. L., Shu, A. P., Xu, X. L., Yang, Q. K., Yu, B.: Soil erodibility and its estimation for agricultural soils in
440 China, *J. Arid Environ.*, 72, 1002–1011, 2008.

441 Zhao, M. Y., Zhao, W. W., Liu, Y. X.: Comparative analysis of soil particle size distribution and its influence
442 factors in different scales: a case study in the Loess hilly-gully area, *Acta Ecologica Sinica*, 35, 4625–4632,
443 2015. (in Chinese with English abstract).

444 Zhao, W. W., Fu, B. J., Chen, L. D.: A comparison between soil loss evaluation index and the C-factor of RUSLE:
445 a case study in the Loess Plateau of China, *Hydrol. Earth Syst. Sci.*, 16, 2739–2748, 2012.
446

Table 1 Landscape and soil characteristics in the study area

Vegetation type/type	Natural vegetation		Artificially managed vegetation			Artificially restored vegetation		
	NG	FL	AO	PG	SB	CK	BL	DP
Sampling Sample number	25	22	10	11	15	18	38	12
Ele (m)	1392.60	1380.14	1370.10	1401.00	1435.67	1350.61	1326.54	1377.58
SG (°)	16.72	6.27	19.90	11.91	16.40	17.56	27.24	24.17
Cla (%)	7.44	7.93	7.05	7.88	6.70	7.21	8.30	8.34
Sil (%)	45.08	52.63	48.57	42.73	45.05	48.08	51.75	49.69
San (%)	47.48	39.44	44.38	49.39	48.25	44.71	39.95	41.97
OM (g/kg)	7.04	5.31	5.75	6.30	8.91	13.30	8.10	5.99
SBD (g/cm ³)	1.26	1.29	1.25	1.28	1.23	1.26	1.23	1.26
Por (%)	0.48	0.46	0.48	0.47	0.48	0.49	0.49	0.49
AAR (mm)	473.99	479.01	479.85	471.75	476.44	474.66	474.43	472.58
VC (%)	57.36	53.14	39.70	67.82	66.07	46.28	59.58	33.75
AB (g/m ²)	28.96	95.61	12.24	73.56	28.59	45.63	23.92	16.20
VH (m)	0.59	1.83	3.58	0.67	2.16	1.81	11.49	3.02
LB (g/m ²)	15.70	—	8.64	12.06	25.10	34.05	72.50	14.44
PD (/m ²)	—	—	30.50	—	262.40	131.89	58.66	36.17
Cro (cm)	—	—	398.39	—	184.85	205.20	448.72	293.40
BD (cm)	—	—	6.32	—	3.76	1.59	10.16	4.98
BN	—	—	10.17	—	—	27.88	12.86	8.13

448 Annotation: NG [refers to notes](#) native grassland, AO [refers to notes](#) apple orchard, FL [refers to notes](#) farmland, PG [refers to notes](#) pasture
449 grassland, SB [refers to notes](#) sea buckthorn, CK [refers to notes](#) *Caragana korshinskii*, DP [refers to notes](#) David's peach, BL [refers to notes](#) black
450 locust, Ele [refers to notes](#) elevation, SP [refers to notes](#) slope position, SA [refers to notes](#) slope aspect, SG [refers to notes](#) slope gradient, SS [refers](#)
451 [to notes](#) slope shape, Cla [refers to notes](#) clay, Sil [refers to notes](#) silt, San [refers to notes](#) sand, OM [refers to notes](#) organic matter, SBD [refers](#)
452 [to notes](#) soil bulk density, Por [refers to notes](#) porosity, AAR [refers to notes](#) average annual rainfall, VC [refers to notes](#) vegetation coverage, AB
453 [refers to notes](#) aboveground biomass, VH [refers to notes](#) vegetation height, LB [refers to notes](#) litter biomass, PD [refers to notes](#) plant density, Cro
454 [refers to notes](#) crown, BD [refers to notes](#) basal diameter, and BN [refers to notes](#) branch number.

456 **Table 2** Statistics of soil erodibility in the Ansai watershed

<u>Methods</u> <u>Method</u>	Mean	Max	Min	Median	SD	<u>Skewn</u> <u>ess</u> <u>Skew</u>	<u>Kurt</u> <u>Kurt</u> <u>osis</u>	Cv
EPIC	0.046	0.060	0.032	0.045	0.005	0.408	0.946	0.109
NOMO	0.073	0.092	0.046	0.074	0.008	-0.447	0.956	0.110
M-NOMO	0.075	0.088	0.047	0.075	0.005	-1.079	4.353	0.067
Torri	0.053	0.066	0.009	0.053	0.006	-2.639	16.872	0.113
Shirazi	0.033	0.044	0.018	0.033	0.006	0.059	0.009	0.182

457 Annotation: EPIC ~~refers to~~notes the erosion-productivity impact model, NOMO ~~refers to~~notes the nomograph equation, M-NOMO ~~refers to~~notes
458 the modified nomograph equation, Torri ~~refers to~~notes the K value estimation model established by Torri, Shirazi ~~refers to~~notes the K value
459 estimation model established by Shirazi, SD ~~refers to~~notes the standard deviation, ~~Skew refers to the~~ and ~~Skewness~~, Kurt ~~refers to the~~ kurtosis, Cv
460 ~~refers to~~notes the coefficient of variation, and P ~~refers to~~ p-value of Kolmogorov-Smirnov test.

461 _____

462 **Table 3** Principal component analysis (PCA) of environmental attributes

Vegetation type type	Main influencing factors
Farmland	SS, SP, SG
Apple orchard	PD
Native grasses grasslands	SG, Ele
Pasture grasses grasslands	—
Sea buckthorn	AB, SG, PD
<i>Caragana korshinskii</i>	AAR, Ele
Black locust	SG, SP, Ele, LB, SBD, VC
David's peach	Cro, VH, BD, VC

463 Annotation: SS ~~refers to~~~~notes~~ slope shape, SP ~~refers to~~~~notes~~ slope position, SG ~~refers to~~~~notes~~ slope gradient, PD ~~refers to~~~~notes~~ plant density,

464 Ele ~~refers to~~~~notes~~ elevation, AB ~~refers to~~~~notes~~ aboveground biomass, AAR ~~refers to~~~~notes~~ average annual rainfall, LB ~~refers to~~~~notes~~ litter

465 biomass, SBD ~~refers to~~~~notes~~ soil bulk density, VC ~~refers to~~~~notes~~ vegetation coverage, Cro ~~refers to~~~~notes~~ crown width, VH ~~refers to~~~~notes~~

466 vegetation height, and BD ~~refers to~~~~notes~~ basal diameter.

467

468

469

Table 4 Suggested soil erodibility estimation models in China

Study area	optimal models Optimal model(s)	References
Hilly area of Chinese China's subtropical zone	Torri	Zhang et al., 2009
Purple hilly region in of Sichuan Basin	EPIC and NOMO ₇	Shi et al., 2012
typical Typical black soil region in Northeast China	EPIC and NOMO ₇	Wang et al., 2012
Hilly and gully area of Chinese China's Loss Loess Plateau	Torri and Shirazi	Lin et al., 2017
Hilly and gully area of Chinese China's Loss Loess Plateau	Shirazi	Wei et al., 2017

470

471

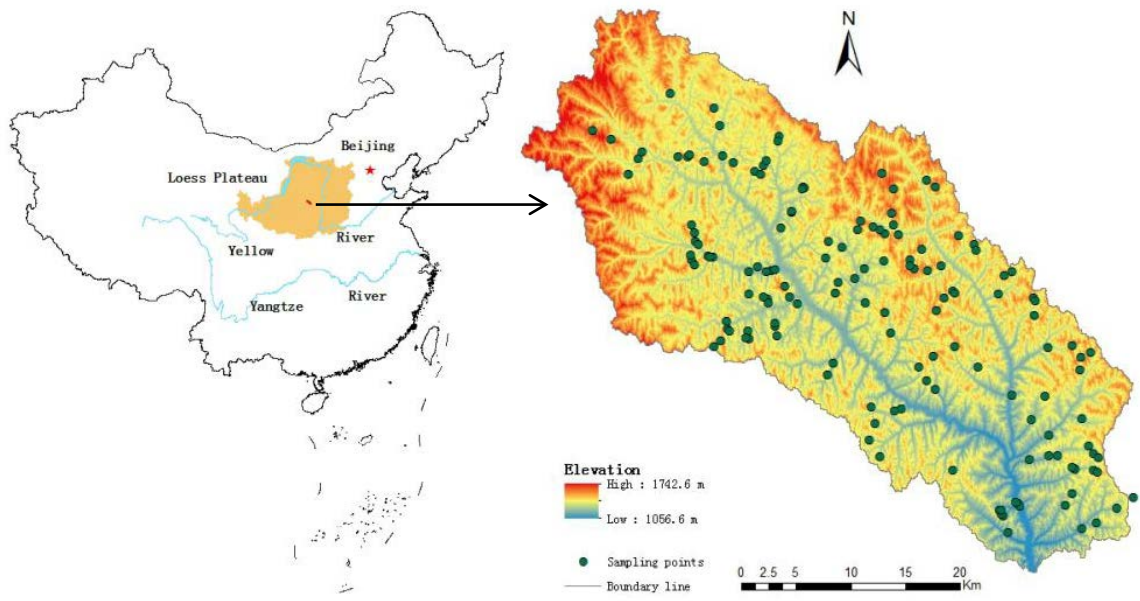
472 **Fig. 1** ~~Location~~Locations of the study area and the sampling points

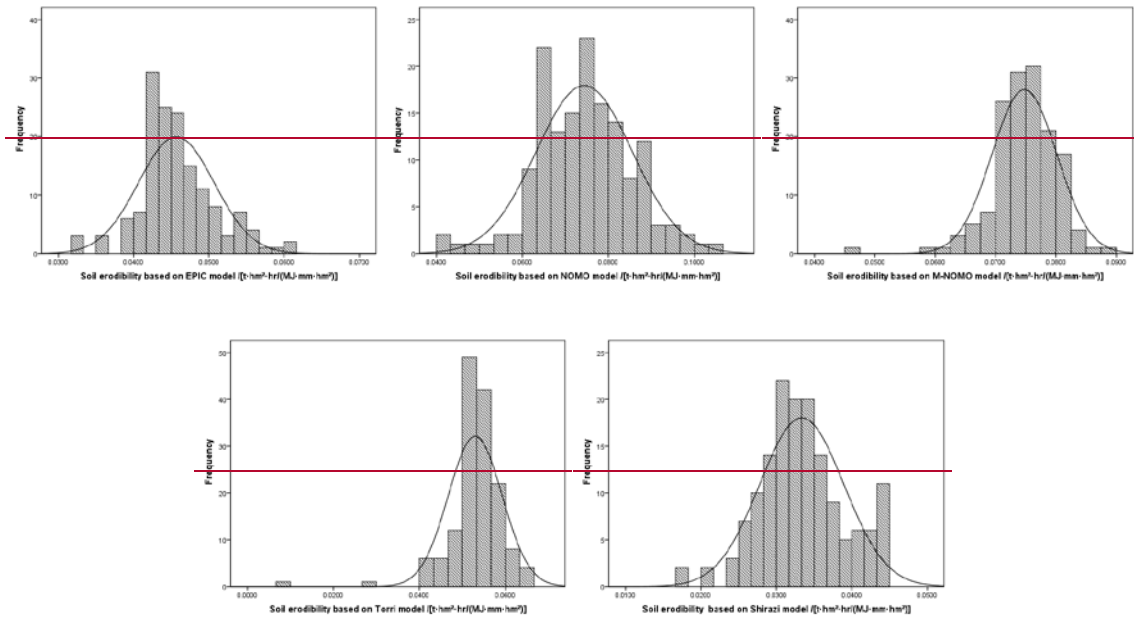
473 **Fig. 2** ~~Frequency distributions of soil erodibility~~

474 **Fig. 3** Taylor diagram ~~were~~-used to compare ~~the estimating~~estimated K values among models

475

476 Figure 1





480

481

482

